

Enfoque UTE
ISSN: 1390-6542
enfoque@ute.edu.ec
Universidad UTE
Ecuador

Álava Bermeo, Manuel; García Solórzano, Antony; Pacheco Gil, Henry; Delgado Marcillo., Cristhian Model for estimating soil chemical properties with RGB drone images Enfoque UTE, vol. 15, núm. 4, 2024, Octubre-Diciembre, pp. 19-26 Universidad UTE Ecuador

DOI: https://doi.org/10.29019/ enfoqueute.1078

Disponible en: https://www.redalyc.org/articulo.oa?id=572279095003







Página de la revista en redalyc.org



Sistema de Información Científica Redalyc Red de revistas científicas de Acceso Abierto diamante Infraestructura abierta no comercial propiedad de la academia

Model for estimating soil chemical properties with RGB drone images

Manuel Álava Bermeo¹, Antony García Solórzano², Henry Pacheco Gil³, Cristhian Delgado Marcillo⁴

Abstract — Precision agriculture optimizes crop management by providing accurate data on soil chemical properties, thereby improving agricultural productivity and sustainability. This study aims to develop models to estimate soil chemical properties, such as pH, electrical conductivity (EC), and organic matter (OM), by analyzing drone-captured RGB images. The methodology included photogrammetric flights with a DJI Phantom 4 Pro drone equipped with a 20 Mpx camera and simultaneous sampling, laboratory analysis and on-site measurements, with Royal Eijkelkamp EC meter set voor grond multiparameter sensors and pH meter set for soil and water. The aerial images were processed with the PIX4Dmapper software, to generate the orthophoto and spectral bands. With the resulting orthophoto of 1.6 cm/pixel, eight spectral indices were calculated, using the spatial analysis tools of ArcGIS software. The in situ results showed an average pH value of 5.83, indicating a slightly acidic soil, and an EC of 1.09 dS/m, suggesting a soil with a low concentration of dissolved salts. Laboratory analyses showed a medium-high content of OM, with an average of 5.19 %. A strong correlation was found between OM and pH_index with coefficients of determination R²=0.55, while moderate correlations were also observed between pH with pH_index and EC with sal_index6 with coefficients of determination R^2 =-0.39 and R^2 =0.42 respectively. The aforementioned results allowed the generation of two models for the estimation of these variables from RGB images.

Keywords: precision agriculture; spectral indices; Phantom 4 Pro; PIX4Dmapper, ArcGIS.

Resumen — La agricultura de precisión optimiza la gestión de cultivos al proporcionar datos precisos sobre las propiedades químicas del suelo, mejorando así la productividad y sostenibilidad agrícola. Este estudio tiene como objetivo desarrollar modelos para estimar propiedades químicas del suelo, como pH, conductividad eléctrica (CE) y materia orgánica (MO), mediante el análisis de imágenes RGB capturadas por dron. La metodología incluyó vuelos fotogramétricos con un dron DJI Phantom 4 Pro equipado con una cámara de 20 Mpx y la toma simultánea de muestras de análisis de laboratorio y mediciones in situ, con sensores multiparámetros Royal Eijkelkamp EC meter set voor

Manuscript Received: 09/08/2024

Revised: 02/09/2024 Accepted: 09/09/2024

DOI: https://doi.org/10.29019/enfoqueute.1078

grond y pH meter set for soil and water. Las imágenes aéreas fueron procesadas con el software PIX4Dmapper, para generar la ortofoto y bandas espectrales. Con la ortofoto resultante de 1.6 cm/píxel, se calcularon ocho índices espectrales, usando las herramientas de análisis espacial del software ArcGIS. Los resultados in situ mostraron un valor promedio de pH de 5.83, indicando un suelo ligeramente ácido, y una CE de 1.09 dS/m, sugiriendo un suelo con baja concentración de sales disueltas. Los análisis de laboratorio evidenciaron un contenido medio-alto de MO, con un promedio de 5.19 %. Se encontró una correlación fuerte entre la MO y el pH_index con coeficientes de determinación R²=0.55, por su parte también se observaron correlaciones moderadas entre pH con el pH_index y CE con el sal_index6 con coeficientes de determinación R²=-0.39 y R²=0.42 respectivamente. Los resultados mencionados permitieron generar dos modelos para la estimación de estas variables a partir de imágenes RGB.

Palabras Clave: agricultura de precisión; índices espectrales; Phantom 4 Pro; PIX4Dmapper, ArcGIS.

I. INTRODUCTION

AGRICULTURE is an essential activity for the survival of the human being, which significantly influences the economy of Ecuador with 10 % of GDP, promoting development and reducing poverty contributing 19 % to the generation of employment [1].

By using advanced spatial analysis tools, such as Geographic Information Technologies (GIT), agriculture and soil management specialists can make informed decisions to optimize agricultural practices [2].

Soil quality is fundamental for agricultural productivity, it is a complex ecosystem [3], it needs to evaluate chemical parameters such as organic matter (OM), hydrogen potential (pH) and electrical conductivity (EC) to improve its structure, retain water and nutrients [4].

Understanding pH, electrical conductivity (EC), and organic matter (OM) is crucial for assessing soil quality in agriculture. pH affects nutrient availability and plant growth, while EC indicates salt concentration, which can impact water and nutrient uptake. OM improves soil structure, water retention, and microbial biodiversity. Together, these parameters enable more precise soil management, optimizing conditions for healthy and sustainable crop development [5].

The limitation in determining the chemical variables of the soil lies in the constant need to evaluate the productive capacity of the soil through exhaustive laboratory analyses [6]. However, this practice faces several obstacles, as it is costly, time-consuming in processing samples and, in many cases, is not carried out due to a lack of knowledge on the part of producers [7].

^{1.} Manuel Álava Bermeo. Filiation: Universidad Técnica de Manabí. Email: malava7130@utm.edu.ec, ORCID: https://orcid.org/0009-0008-4027-4950.

^{2.} Antony García Solórzano. Filiation: Universidad Técnica de Manabí. Email: agarcia6793@utm.edu.ec, ORCID: https://orcid.org/0009-0003-0124-2423

^{3.} Henry Pacheco Gil. Filiation: Universidad Técnica de Manabí. Email: henry.pacheco@utm.edu.ec, ORCID: https://orcid.org/0000-0002-9997-9591

^{4.} Cristhian Delgado Marcillo. Filiation: Universidad Técnica de Manabí. Email: cristhian.delgado@utm.edu.ec, ORCID: https://orcid.org/0009-0006-7248-6718

To address this problem, it is proposed to use spectral calculation from the RGB bands (corresponding to the red, green and blue wavelengths), of aerial images captured by low-cost drones, with the aim of developing a model adapted to local conditions that provides reliable and fast data on key chemical properties of the soil. Such as pH, electrical conductivity and organic matter content [8].

The research by Krestenitis et al. [9] presents an innovative path planning method for UAVs in precision agriculture. The goal is to acquire high-quality data in the shortest possible flight time by adjusting the UAV's speed.

The integration of remote sensing technologies is presented as a promising tool to study the chemical properties of soil, offering accurate and relevant data [10].

Petrovic's research confirms that Agriculture 5.0 has now begun with the widespread use of robotic systems in various field operations, supported by the Internet of Things (IoT), autonomous self-driving devices (robots and drones), and artificial intelligence [11].

Precision agriculture in Ecuador is used in the floriculture, banana, and sugar sectors, mainly for the implementation of automated irrigation systems, pest monitoring and control, moisture management, and ventilation. In this context, drones are used for pest detection and monitoring, as well as for topographic surveys in order to optimize crop management [12].

The implementation of TIG in the study of soil chemical properties involves the acquisition, organization and analysis of detailed geospatial data on pH, EC and OM, through the use of specialized tools that allow the generation of layers of information and the performance of spatial analyses to identify patterns and distributions where modeling techniques are used to predict the distribution of soil properties in unsampled areas. In order to optimize agricultural practices, improve crop management and maximize productivity in an efficient and sustainable way [13].

UAV equipped with high-definition cameras and sensors like LiDAR, are essential tools in agricultural remote sensing. They enable georeferencing data and creating accurate maps of crop health, estimating bio-physical characteristics such as growth and yield. They offer an advanced alternative to traditional field exploration, providing detailed views at the plant and leaf level due to their high resolution and segmentation algorithms [14].

Mao et al. [15], point out that the use of low-end unmanned aerial vehicles (UAVs) has many advantages, such as low cost, high resolution, and considerable spatial coverage giving value to remote sensing data. Remote sensing is based on collecting data from various aerial photographs at different spectral ranges [16].

The next innovation in smart UAVs aims to transform agriculture with cost savings and increased yields. However, they face cybersecurity risks, which could be mitigated through Blockchain and 5G networks [17].

Tan et al. [18], highlights that drones equipped with hyperspectral sensors are crucial for agricultural monitoring, capturing changes in vegetation and soil, and providing spectral information to monitor salinity. The use of regression algorithms, such as Random Forest, has matured as an effective solution for predicting properties like soil salinity, handling nonlinear fitting problems and high-dimensional data.

In the context of soil analysis, the technology of RGB image analysis algorithms is effectively deployed. This approach involves the application of statistical and mathematical methods to the images acquired by a drone equipped with an RGB digital camera. Through this process, the precise identification and quantification of the wavelengths contained in the images is achieved, thus allowing a detailed analysis of soil properties in a non-invasive and reliable way [19].

Recent research by Lintes et al. [20] developed a radar method using two unmanned aerial vehicles in a bistatic system. This system irradiates the Earth's surface obliquely to create the Brewster effect, which enhances the reflection of radio signals from subsurface horizons, allowing for the determination of their physical and chemical parameters.

In a study by Ngabire et al. [21], in the Shiyang River basin, remote sensing was applied to analyze soil salinization in arid and semi-arid environments. A multiple linear regression model was used with 80 samples, divided for training and validation using the Kennard-Stone algorithm. Multicollinearity identification was performed with the variance inflation factor (VIF), adjusting covariates to ensure proper model specification. The results showed outstanding performance, with a coefficient of determination R²=0.898 and a mean square error (RMSE) of 1.653. These findings are of vital importance to support the integration of remote sensing into the analysis of soil chemical properties.

This soil analysis study focused on addressing the imperative need to efficiently estimate the chemical parameters of the soil through image geoprocessing techniques, taking advantage of remote sensing and RGB digital camera tools. This strategy is based on the precise determination and evaluation of electrical conductivity (EC), pH and organic matter content in the soil, thus offering a significant contribution to the advancement of sustainable management of agricultural resources [22].

II. METHODOLOGY

Location of the study area

This study was carried out on a plot of 0.38 hectares, located in the Lodana parish of the Santa Ana canton belonging to the province of Manabí. Its geographical location is 80°23'13.60"W, 1°10'25.51"S (Fig. 1). The average temperature is 27.6°C and its average annual rainfall is 83.60 mm [23].

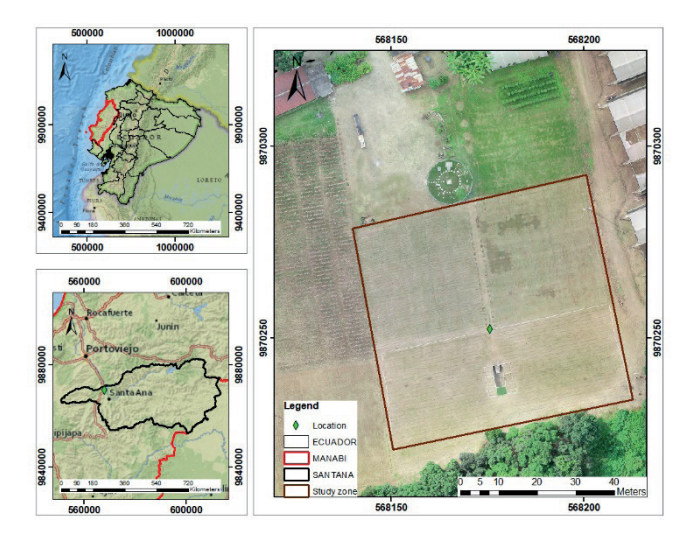


Fig 1. Location of the study area

On-site measurements and field sampling.

To define the sampling points systematically, a system of diagonal transects [24] was used in the study area as shown in (Fig. 2). A total of 45 sampling points were surveyed Between July 20 and 22, 2023, coinciding with the end of the drought period in the area, which were georeferenced by means of a topographic implement called RTK (Real Time Kinematics) GPS model Topcon GR-5. With the coordinates generated by the RTK, a shapefile vector file was constructed, using ArcGIS software tools. Fields with the variables pH, EC and MO were added to the attribute table of the shapefile file with the data measured in the field and laboratory.



Fig. 2. Orthophoto of the area where the soil samples were obtained.

At each sampling point, the chemical parameters electrical conductivity (EC) and hydrogen potential (pH) were measured in situ using EC-pH meters [25] multiparameter sensors, which are equipment that have an automatic calibration and allow measuring pH on a scale of 0 to 14 with an accuracy of 0.01 pH units while for EC it performs it in a measurement range 0.1 μ S/cm to 200 mS/cm with an accuracy of 0.01 μ S/cm (Fig. 3).

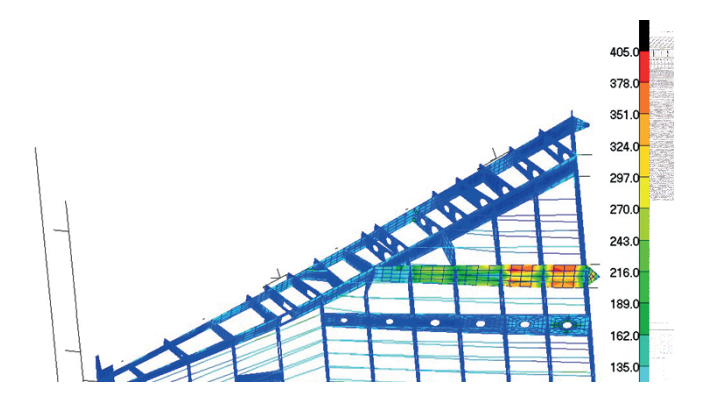


Fig. 3. On-site sampling with electrical conductivity (EC) and hydrogen potential (pH) meters.

Before the on-site measurements were made, the ground was prepared by tilling the soil, with a metal tip, to loosen the first 5 cm of the surface layer, thus facilitating the correct insertion of the sensor head. Once the sensor was inserted, it was waited for it to stabilize before proceeding to record the electrical conductivity (EC) and hydrogen potential (pH) data. Each parameter was measured in three replications and the average value obtained was recorded.

Field sampling involved the extraction of soil samples, each of approximately 500 gr, using a field drill to reach depths of 20 and 40 cm, which was mixed and homogenized to generate a composite sample at each sampling site. The samples were deposited in duly labeled sample holder sleeves, and transported to the water and soil laboratory of the Faculty of Agricultural Engineering of the Technical University of Manabí for the respective analyses.

Laboratory tests

The laboratory analysis consisted of the determination of soil organic matter (OM) content by means of the loss-on-ignition (LOI) or gravimetric method proposed by Schulte and Hopkins [26]. To determine OM, samples were kiln dried at 105°C for 24 hours, cooled in a desiccator and then weighed 5g of sample and placed in crucibles before being calcined at 600°C for 2h in a Lindberg/blue M muffle furnace. After combustion, the samples were cooled in a desiccator and re-weighed on an analytical balance. With these values, the percentage of OM was calculated using [1].

$$LOI = \frac{(PSS_{105^{\circ}C} - PSI_{600^{\circ}C})}{(PSS_{105^{\circ}})} * 100$$
(1)

Where PSS represents the dry weight of the soil and PSI the weight after ignition.

Aerial image processing with drone

The aerial image capture was done with the DJI Phantom 4 Pro drone, equipped with a 20 MPX RGB camera, capable of detecting the wavelengths of the color red, green, and blue in the visible electromagnetic spectrum [13]. The flight planning was carried out using the DJI GO4 software, this software allowed to define the region of interest, the flight height was 60

m, speed 3.3m/sec, the pixel resolution was 1.5 cm/pixel, the superposition of images, as well as the strategic choice of take-off and landing points.

The RGB images obtained with the drone were subjected to an analysis process using the PIX4Dmapper photogrammetry software. This process was carried out in the Scientific Model and Calculation laboratory of the Faculty of Agricultural Engineering of the UTM, with a high-end computer.

The processing methodology encompassed the import of images and coordinates of the control points, as well as the implementation of necessary adjustments in each phase of the process. These adjustments were executed in order to ensure exhaustive control over the quality of the data obtained through image processing by means of GIS [27], this process allowed the generation of quality photogrammetric products such as orthophoto, RGB bands, digital surface and terrain models, as well as the 3D point cloud.

With the RGB spectral bands, the respective calculation of the indices shown in Table I was carried out. These have been reported in the literature as medium-power indices [28], [29] and [30], to determine chemical parameters of the soil (pH, salinity and organic matter), because they have only three bands of the electromagnetic spectrum [31].

TABLE I SPECTRAL INDICES TO ESTIMATE SOIL CHEMICAL PROPERTIES

Parameter	Index
pH_index	(Red/Green)/Blue
sal_index1	√Blue * Red
sal_index2	$\sqrt{Green*Red}$
sal_index3	$\sqrt{Green^2*Red^2}$
sal_index4	Blue/Red
sal_index5	(Green * Red)/Blue
sal_index6	(Blue * Red)/Green
carb_index	(-0.008 * Red) + (-0.008 * Green) + (0.008 * Blue) + 0.807

Statistical analysis

IBM SPSS Statistics (Statistical Package for Social Sciences) statistical software tools were used to perform correlation and regression analyses, in order to model and relate the data obtained in the field and laboratory such as pH, EC, MO and spectral indices. Due to the nature of the data, Pearson's correlation was used, which varies between -1 and 1 evidenced in Table II, quantifies the strength and direction of the linear relationship between two continuous variables; it is preferred for analyses where a precise linear relationship between variables is anticipated [32].

TABLE II
PEARSON'S CORRELATION COEFFICIENT

Condition	Degree of correlation
0.00 - 0.10	Non-existent correlation
0.10- 0.29	Weak correlation
0.30 - 0.50	Moderate correlation
0.50 - 1.00	Strong correlation

III. RESULTS AND DISCUSSION

Chemical parameters of the soil

Soil chemical parameters were determined, including pH, electrical conductivity (EC), and organic matter (OM) content. According to the values in the table indicated, the classification of electrical conductivity exhibits non-saline characteristics, with average values of 1.09 dS/m, belonging to the category of soils with low concentration of dissolved salts according to the classification of [33], shown in Table III.

TABLE III CLASSIFICATION OF THE ELECTRICAL CONDUCTIVITY OF SOIL

dS/m	Classification
< 2	Not saline
2 a 4	Slightly saline
4 a 8	Moderately saline
8 a 16	Strongly saline
> 16	Extremely saline

Based on the soil pH classification presented in Table IV, the soil was determined to be slightly acidic, with an average value of 5.86 according to the classification of [34]. This value indicates moderate acidity, which can influence nutrient availability and soil microbial activity, which are crucial for agricultural productivity and ecosystem health [22].

TABLE IV
CLASSIFICATION OF SOIL HYDROGEN POTENTIAL

pН	Classification
0.00 a 4.50	Very acid
4.50 a 5.50	Moderately acidic
5.50 a 6.50	Slightly acidic
6.50 a 7.50	Neutral
7.50 a 8.50	slightly alkaline
8.50 a 9.50	Moderately alkaline
9.50 a 14.00	Very alkaline

Regarding organic matter, an average of 5.19 % of organic matter was found in the soil, considered a medium-high percentage, according to the classification shown in Table V, [35], it is beneficial due to its positive effects on soil structure, water and nutrient retention, as well as on the promotion of microbiological activity [31].

TABLE V
PERCENTAGE OF SOIL ORGANIC MATTER

%	Range	
0.00 -1.00	Low	
1.00-2.50	Medium bass	
2.50-4.00	Half	
4.00-5.50	Medium high	
5.50-7.00	High	
7.00-8.50	Very high	
8.50-10.00	Exceptionally high	

Aerial images and spectral indices.

Fig. 4 shows the calculation of the spectral indices that yielded the best results. The pH_index stands out for indicating the degree of alkalinity of the soil, while the sal_index6 reflects the content of dissolved salts.

Orthophoto resolution and quality

The orthophoto acquired on July 20, 2023 at 10:30 AM presents a high quality thanks to its spatial resolution of 1.6 cm/pixel, which allows an exceptional level of detail in the repre-

sentation of the terrain. The image covers an area of 0.44 hectares, captured under optimal atmospheric conditions, with clear skies, which ensures superior clarity and sharpness in the RGB bands used. In addition, the orthophoto is fully compatible and integrated with ArcGIS software because it is generated in a GEOTIFF format, facilitating its use in GIS applications and ensuring its efficiency in geospatial analysis.

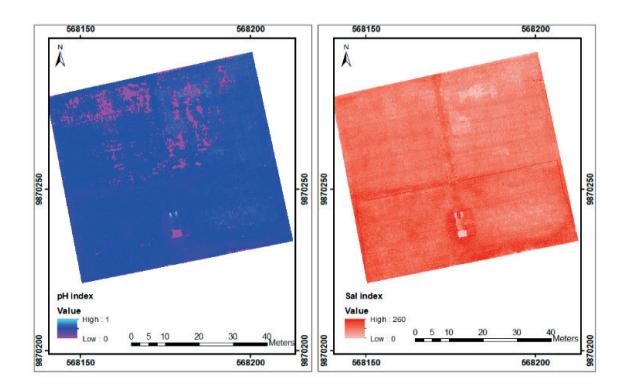


Fig. 4. Processing of aerial images and indexes

Index statistics

Table VI shows the soil data obtained in the field and laboratory, as well as the spectral indices calculated with the photogrammetric products.

 ${\it TABLE\ VI}$ FIELD, LABORATORY AND PHOTOGRAMMETRIC PRODUCT VALUES

Data	CE	pН	МО	Red	Green	Blue	ph_index	sal_index1	sal_index2	sal_index3	sal_index4	sal_index5	sal_index6	carb_index
1	1.50	6.20	6.00	221	212	192	0.00521	205.99	216.45	46852	-0.0702	244.02	200.15	-1.121
2	1.20	5.70	4.00	212	204	177	0.00565	193.71	207.96	43248	-0.0900	244.34	183.94	-1.105
3	1.20	5.80	4.00	211	204	171	0.00585	189.95	207.47	43044	-0.1047	251.72	176.87	-1.145
4	0.90	5.80	4.00	196	192	150	0.00667	171.46	193.99	37632	-0.1329	250.88	153.13	-1.097
5	0.90	5.30	6.00	195	190	153	0.00654	172.73	192.48	37050	-0.1207	242.16	157.03	-1.049
6	1.10	5.40	6.00	204	195	175	0.00571	188.94	199.45	39780	-0.0765	227.31	183.08	-0.985
7	0.90	5.30	6.00	152	143	125	0.00800	137.84	147.43	21736	-0.0975	173.89	132.87	-0.553
8	1.00	5.30	2.00	204	195	175	0.00571	188.94	199.45	39780	-0.0765	227.31	183.08	-0.985
9	1.00	5.40	4.00	217	211	190	0.00526	203.05	213.98	45787	-0.0663	240.98	195.40	-1.097
10	1.50	6.30	6.00	208	196	175	0.00571	190.79	201.91	40768	-0.0862	232.96	185.71	-1.025
11	1.20	5.70	6.00	207	200	172	0.00581	188.69	203.47	41400	-0.0923	240.70	178.02	-1.073
12	1.30	5.50	5.49	189	182	151	0.00662	168.94	185.47	34398	-0.1118	227.80	156.81	-0.953
13	0.60	6.60	2.45	185	186	161	0.00000	172.58	185.50	34410	-0.0694	213.73	160.13	-0.873
14	1.00	6.40	5.47	193	184	162	0.00617	176.82	188.45	35512	-0.0873	219.21	169.92	-0.913
15	1.30	6.40	5.68	179	171	149	0.00671	163.31	174.95	30609	-0.0915	205.43	155.97	-0.801
16	1.10	6.20	5.25	183	178	152	0.00658	166.78	180.48	32574	-0.0925	214.30	156.27	-0.865
17	1.00	6.20	5.39	193	187	154	0.00649	172.40	189.98	36091	-0.1124	234.36	158.94	-1.001
18	0.80	5.50	5.38	211	205	168	0.00595	188.28	207.98	43255	-0.1135	257.47	172.92	-1.177

Data	CE	pН	МО	Red	Green	Blue	ph_index	sal_index1	sal_index2	sal_index3	sal_index4	sal_index5	sal_index6	carb_index
19	1.10	6.00	5.57	204	201	181	0.00553	192.16	202.49	41004	-0.0597	226.54	183.70	-0.985
20	1.10	5.80	6.15	178	173	162	0.00617	169.81	175.48	30794	-0.0471	190.09	166.68	-0.705
21	1.30	5.90	5.69	187	187	168	0.00595	177.25	187.00	34969	-0.0535	208.15	168.00	-0.841
22	1.00	6.00	6.32	183	180	169	0.00592	175.86	181.49	32940	-0.0398	194.91	171.82	-0.745
23	1.00	6.00	6.17	160	158	141	0.00709	150.20	159.00	25280	-0.0631	179.29	142.79	-0.609
24	1.20	6.00	5.46	190	183	168	0.00595	178.66	186.47	34770	-0.0615	206.96	174.43	-0.833
Averages	1.09	5.86	5.19	194.25	188.21	164.21	0.01	178.55	191.20	36820.13	-0.08	223.10	169.49	-0.94

5. Correlation analysis and regression models

Pearson's correlation coefficients are shown in Table VII.

TABLE VII CORRELATIONS

	Red	Green	Blue	ph_index	sal_index1	sal_index2	sal_index3	sal_index4	sal_index5	sal_index6	carb_index
CE	.303	.227	.354	.305	.342	.267	.271	.135	.118	,421*	161
pН	-,369*	-,350*	-,339*	394	051	093	113	.222	168	027	.151
MO	279	316	199	,545**	246	298	293	.122	321	168	.324

In relation to soil organic matter (OM) content, a strong correlation was observed with the pH index (pH_index), evidenced by a coefficient of determination R²=0.55 and RMSE 0.72 (Fig. 6). This finding suggests that pH_index is closely related to the content of OM in the soil. The significance of the data obtained reinforces the usefulness of the pH_index as a reliable indicator to estimate the percentage of OM in the soil. This robust correlation highlights the importance of this index in the assessment of soil fertility and health, providing a valuable tool for agricultural management.

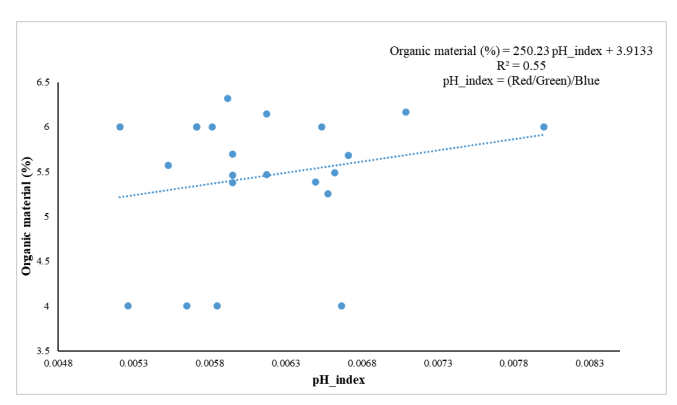


Fig. 6. Scatterplot of the correlation between WM and pH index.

Regarding pH, a moderate correlation was observed, with an R^2 =-0.39 and RMSE 0.35 between pH and pH index (Fig. 7). This indicates that an increase in pH is associated with a decrease in the pH index, revealing an inverse relationship that underscores the significant influence of pH on the characteristics assessed by the index.

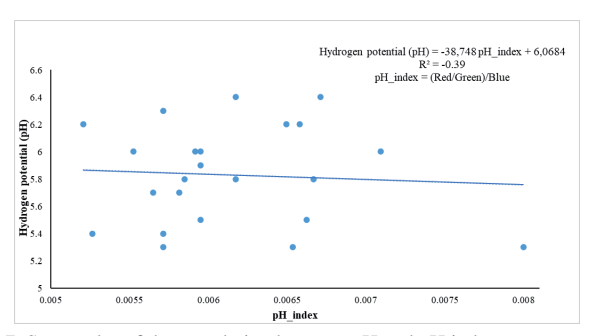


Fig. 7. Scatterplot of the correlation between pH and pH index.

In relation to electrical conductivity (EC), a moderate correlation was observed with the salinity index (sal_index6), with a coefficient of determination R²=0.42 and RMSE 0.17 (Fig. 8). This result indicates a significant relationship between soil EC and sal_index6, suggesting that this index may be a useful indicator for estimating the soluble salt content of soil. The moderate correlation observed highlights the relevance of this index in the evaluation of soil chemical properties.

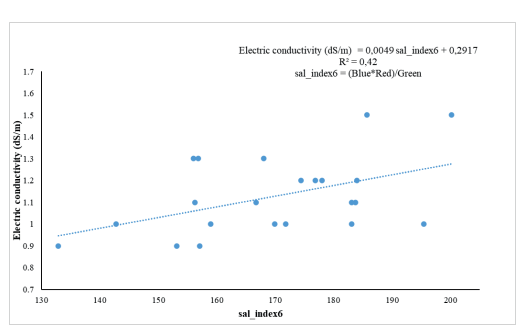


Fig. 8. Scatterplot of the correlation between electrical conductivity and sal_index6.

The simple linear regression estimation model presents some limitations that may be related to the presence of multi-collinearity or outliers. To improve the implementation of these models, it is suggested to incorporate artificial intelligence algorithms, such as artificial neural networks [36].

The implementation of RGB spectral indices for soil analysis and estimation of their chemical properties has significant advantages over the most advanced multispectral techniques. RGB sensors are much cheaper and therefore accessible to a wide audience, from small farmers to researchers with limited budgets. In addition, these sensors are often available in common devices such as smartphones and drones, making them easy to use in various agricultural and research applications [37].

The use of this technique is simpler to implement, as these sensors are easier to handle, allowing users to capture and analyze images without the need for specialized equipment. Its accessibility translates into faster processing and analysis, as RGB data is less complex to manage than multispectral data. Algorithms for processing RGB images are simpler and less demanding in terms of computational resources [38].

The images generated by these technologies are easily integrated into common photo analysis platforms and tools, avoiding the need for specialized software, although they do not provide the same spectral depth as advanced sensors, they are effective in detecting visual changes in soil and crops, in addition, these cameras are less sensitive to environmental variations such as humidity and lighting, facilitating the capture of images in various conditions without constant adjustments [39].

IV. CONCLUSION

The average electrical conductivity of the soil was 1.09 dS/m, indicating non-saline conditions. The soil was determined to be slightly acidic, with an average pH value of 5.86.

The organic matter presented an average of 5.19 %, which is considered within a medium-high range.

Photogrammetric flight generated a high-quality orthophoto with a resolution of 1.6 cm per pixel. Eight RGB spectral indices were calculated, of which only pH_index showed a strong correlation with organic matter, with a coefficient of determination R²=0.54

On the other hand, the sal_index6 and presented a moderate correlation with electrical conductivity (EC), with a coefficient of determination R^2 =0.42.

Additionally, a moderate negative correlation was observed between pH and pH index, with an R^2 =-0.39.

The rest of the indices studied showed weak relationships with respect to the chemical properties of the soil.

Three models were proposed to estimate soil chemical properties from spectral indices as useful indicators that can result in time and money savings, as well as a decrease in the environmental impacts of agricultural activities.

The results obtained confirm the potential of drone-captured RGB images as a cost-effective and accessible alternative to traditional methods of soil chemical analysis.

It is essential to validate these models in various agricultural environments to ensure their applicability and accuracy

under different agroecological conditions. This validation will extend the robustness and reliability of the proposed approach, allowing its widespread adoption in different productive areas.

REFERENCES

- [1] L. Toledo, R. L. Changoluisa Chiguano and O. Viteri Salazar, "Influencia de la agricultura en la economía y su contraste frente a los objetivos de desarrollo sostenible: caso Ecuador," *Revista Científica de Ciencias Sociales y Humanas*. vol. 2, no. 83, pp. 28-49, 2023. https://doi.org/10.33324/uv.v2i83.697
- [2] F. González Soto, D. Ullón and J. Loján, "Análisis multitemporal de cambios de uso del suelo en la isla Santa Cruz, archipiélago de las Galápagos, periodo 1991-2023," *Revista Ciencia y Tecnología*, vol. 17, no. 1, pp. 1-9, 2024. https://doi.org/10.18779/cyt.v17i1.521
- [3] R. Vicente Salar, M. Castelló Bueno, S. Logan de la Rosa and J. C. Padró García, "Efecto de los usos y las cubiertas del suelo y las políticas ambientales en el comportamiento de las temperaturas superficiales en campus universitarios: El caso de la Universidad Autónoma de Barcelona," Revista Documents d'Analisi Geográfica, vol. 70, no. 2, pp. 261-289, 2024. https://doi.org/10.5565/rev/dag.875
- [4] W. Zárate Martínez, M. Felipe Victoriano, F. E. Martínez Silva, K. Moreno León, J. L., Arispe Vázquez and J. F. Díaz Nájera, "Propiedades químicas del suelo y calidad del agua en Miahuatlán de Porfirio Díaz y Ejutla de crespo, Oaxaca, México," *Revista de Ecosistemas y Recursos Agropecuarios*, vol. 11, no. 1, pp. 2-10, 2024. https://doi.org/10.19136/era.a11n1.3948
- [5] A. Vélez, M. Vera, S. Valdez, D. Martínez and F. Cutipa, "Methods to determine enzymatic activity in contaminated soils," *South Sustainability*, vol. 5, no. 1, pp. 1-11, 2024. https://doi.org/10.21142/SS-0501-2024-e092
- [6] A. Gonzales and L. Castellanos, "Impacto de diferentes prácticas agrícolas sobre las características fisicoquímicas del suelo: un análisis crítico," Revista Ambiental Agua, Aire y Suelo, vol. 15, no. 1, 90-105, 2024. https://doi.org/10.24054/raaas.v15i1.2916
- [7] R. Enesi, M. Dyck, M. Thilakarathna, S. Strelkov, and L. Gorim, "Calibrated SoilOptix estimates of soil pH and exchangeable cations in three agricultural fields in western Canada implications for managing spatially variable soil acidity". *Journal Heliyon*, vol. 10 no. 17, pp. 1–18, 2024. https://doi.org/10.1016/j.heliyon.2024.e37106
- [8] S. Boubehziz, C. Piccini, M. A. Jiménez González and G. Almendros, "Distribución espacial de los descriptores de calidad del carbono orgánico del suelo que determinan los factores que afectan su secuestro en el Noreste de Argelia", Revista de Gestión Ambiental, vol. 358, pp. 1-10, 2024. https://doi.org/10.1016/j.jenvman.2024.120772
- [9] M. Krestenitis, E. Raptis, A. Kapoutsis, K. Ioannidis, E. Kosmatopoulos and S. Vrochidis, "Overcome the fear of missing out: active sensing UAV scanning for precision agriculture," *Robotics and Autonomous Systems*, pp. 1-13, 2024. https://doi.org/10.1016/j.robot.2023.104581
- [10] J. M. Guzmán Albores, M. de J. Matuz Cruz, J. Y. Arana Llanes, E. López Carrasco, V. Gómez Vázquez and N. González Cárdenas, "Avances y perspectivas de la agricultura de precisión para la sostenibilidad agrícola", XIKUA Boletín Científico de La Escuela Superior de Tlahuelilpan, vol. 12, no. 24, pp. 1-6, 2024. https://doi.org/10.29057/ xikua.v12i24.12790
- [11] B. Petrović, R. Bumbálek, T. Zoubek, R. Kuneš, L. Smutný and P. Bartoš, "Application of precision agriculture technologies in Central Europe-review," *Journal of Agriculture and Food Research*, vol. 15, no. 1, pp. 1-10, 2024, https://doi.org/10.1016/j.jafr.2024.101048
- [12] L. E. Sánchez Palacios, F. R. Martínez Alcivar, S. T. Torres Sánchez, A. C. Lascano Montes and G. N. Terán Guajala, "Agricultura de Precisión en El Ecuador", Ciencia Latina Revista Científica Multidisciplinar, vol. 8, no. 1, pp. 1532-1542, 2024. https://doi.org/10.37811/ cl_rcm.v8i1.9547
- [13] R. Nitin Lilandhar, P. C. Saurabh, "Detección remota (rs), uav/drones y aprendizaje automático (ml) como potentes técnicas para la agricultura de precisión: eficaces aplicaciones en agricultura". *International Research Journal of Modernization in Engineering Technology and Science*, vol. 5, pp. 4375-4395, 2023. https://doi.org/10.56726/irjmets36817

- [14] P. Vigneault, J. Lafond-Lapalme, A. Deshaies, K. Khun, S. de la Sablonnière, M. Filion, L. Longchamps and B. Mimee, "An integrated data-driven approach to monitor and estimate plant-scale growth using UAV", ISPRS Open Journal of Photogrammetry and Remote Sensing, vol. 11, pp. 1-13, 2024. https://doi.org/10.1016/j.ophoto.2023.100052
- [15] Y. Mao et al., "Rapid monitoring of tea plants under cold stress based on UAV multi-sensor data", Computers and Electronics in Agriculture, vol. 213, pp. 1-13, 2023. https://doi.org/10.1016/j.compag.2023.108176
- [16] D. Kaimaris, "Aerial Remote Sensing Archaeology—A Short Review and Applications", Article Land, vol. 13, no. 7, pp. 1-27. 2024. https:// doi.org/10.3390/land13070997
- [17] M. Raj, H. N. B., S. Gupta, M. Atiquzzaman, O. Rawlley, and L. Goel, "Leveraging precision agriculture techniques using UAVs and emerging disruptive technologies," *Energy Nexus*, vol. 14, pp. 1-25, 2024. https://doi.org/10.1016/j.nexus.2024.100300
- [18] J. Tan, J. Ding, Z. Wang, L. Han, X. Wang, Y. Li, Z. Zhang, S. Meng, W. Cai, and Y. Hong, "Estimating soil salinity in mulched cotton fields using UAV-based hyperspectral remote sensing and a Seagull Optimization Algorithm-Enhanced Random Forest Model," *Computers and Electronics in Agriculture*, vol. 221, pp. 1-10, 2024. https://doi.org/10.1016/j.compag.2024.109017
- [19] Y, Han, "Application of Unmanned Aerial Vehicle Remote Sensing for Agricultural Monitoring", E3S Web of Conferences, pp. 1-6, 2024. https://doi.org/10.1051/e3sconf/202455302022
- [20] G. Linets, A. Bazhenov, S. Malygin, N. Grivennaya, S. Melnikov and V. Gorchakov, "Method for remote measurement of specific conductivity and moisture of subsurface soil horizons," *Smart Agri*cultural Technology, vol. 8, pp. 1-9, 2024. https://doi.org/10.1016/j. atech.2024.100503
- [21] M, Ngabire et al., "Mapeo de la salinización del suelo en diferentes tipos de cobertura terrestre arenosa en la cuenca del rio Shiyang: un enfoque de teledetección y regresión lineal múltiple," Remote Sensing Applications: Society and Environment, vol. 28, pp. 1-18, 2024. https://doi.org/10.1016/j.rsase.2022.100847
- [22] O. Yuzugullu, N. Fajraoui and F. Liebisch, "Soil Texture and Ph Mapping Using Remote Sensing and Support Sampling," *IEEE Journal of Selected Topics in Applied Earth Observations and Remote Sensing*, pp. 1-21, 2024. https://doi.org/10.1109/JSTARS.2024.3422494
- [23] INAMHI, "Datos meteorológicos de la estación La Teodomira Manabí, Santa Ana," Inst. Nac. de Meteorología e Hidrología, Manabí, Ecuador, Rep. 2023.
- [24] S. Schweizer Lassaga, "Muestreo y análisis de suelos para diagnóstico de fertilidad," 1ª ed. Reading, MA: M. Mesén Villalobos and L. Ramírez Cartín, 2011. https://www.mag.go.cr/bibliotecavirtual/P33-9965.pdf
- [25] Eijkelkamp, "EC-pH meters", 2024. www.eijkelkamp.com.
- [26] S. Barrezueta Undas, A. Cervantes Alava, M. Ullauri Espinoza, J. Barrera Leon, and A. Condoy Gorotiza, "Evaluación del método de ignición para determinar materia orgánica en suelos de la provincia el Oro-Ecuador", FAVE Sección Ciencias Agrarias, vol. 19, no. 2, pp. 25-36, 2020. https://doi.org/10.14409/fa.v19i2.9747
- [27] L. M. Dos Santos-Tonial, M. Schimit Colla, J. Bassetto Carra, M. Fabris and V. Aparecido de Lima, "Classification and total carbon determina-

- tion of the soils using RGB digital images combined with machine learning", *Communications in Soil Science and Plant Analysis*, vol. 54, no. 2, pp. 1-13, 2023. https://doi.org/10.1080/00103624.2022.2110891
- [28] R. Shrestha Prasad, S. Qasim and S. Bachri, "Investigating remote sensing properties for soil salinty mapping: A case study in Korat province of Thailand," *Environmental Challenges*, vol. 5, pp. 1-10, 2021. https://doi.org/10.1016/j.envc.2021.100290
- [29] Y. K. Sonn et al., "Development of models to estimate total soil carbon across different croplands at a regional scale using RGB photography", International Journal of Environmental Research and Public Health, vol. 19, no. 15, pp. 2-11, 2022. https://doi.org/10.3390/ijerph19159344
- [30] V. Kumar, B. Kumar Vimal, R. Kumar, M. Kumar and K. Vigyan Kendra, Determination of soil pH by using digital image processing technique. *Journal of Applied and Natural Science*, vol. 6, no. 1, pp. 14-18, 2014. https://doi.org/10.31018/jans.v6i1.368
- [31] S. Yeon Kyu et al., Development of Models to Estimate Total Soil Carbon across Different Croplands at a Regional Scale Using RGB Photography. *International Journal of Environmental Research and Public Health*, vol. 19, no. 15, pp. 2-11, 2022. https://doi.org/10.3390/ijerph19159344
- [32] M. F. Ikhwan, W. Mansor, Z. I. Khan, M. K. A. Mahmood, A. Bu-jang, and K. Haddadi, "Pearson Correlation and Multiple Correlation Analyses of the Animal Fat S Parameter", *TEM Journal*, vol. 13 no. 1, pp. 155-160, 2024, https://doi.org/10.18421/TEM131-15
- [33] C. Omuto, R. Vargas, K. Viatkin and Y. Yigini, "Mapeo de suelos afectados por salinidad", Modelo espacial de suelos afectados por salinidad, 2021, http://www.wipo.int/amc/en/mediation/rules
- [34] D. Ibarra Castillo, J. A. Ruiz Corral, D. R. González Eguiarte, J. G. Flores Garnica and G. Díaz Padilla, "Distribución espacial del pH de los suelos agrícolas de Zapopan, Jalisco, México", Agricultura Técnica En México, vol. 35, no. 3, pp. 267-276, 2009.
- [35] N. C. Arzola Pina and J. Machado de Armas,"Soil aptitude for the production of sugarcane. Part I. Calibration in experimental and production conditions," *Centro Agricola*, vol. 42, no. 2, pp. 33-38, 2015. http://cagricola.uclv.edu.cu/descargas/pdf/V42-Numero_2/cag05215.pdf
- [36] G. Mesías Ruiz, J. Peña, A. Castro, I. Borra Serrano and J. Dorado, "Detección y clasificación de malas hierbas mediante drones y redes neuronales profundas: creación de mapas para tratamiento localizado Weed detection and classification using UAVs and deep neural networks: mapping for localized treatment," Revista de Ciencias Agrarias, vol. 47, no. 1, pp. 175-179, 2024,https://doi.org/10.19084/rca.34973
- [37] L. Biró, V. Kozma-Bognár and J. Berke, "Comparison of RGB Indices used for Vegetation Studies based on Structured Similarity Index (SSIM)," *Journal of Plant Science and Phytopathology*, vol. 8, no. 1, pp. 007-012, 2024, https://doi.org/10.29328/journal.jpsp.1001124
- [38] A. Dwi Priyo, R. Isnain Rachmanto, Mujiyo and Komariah, "The accuracy of soil moisture prediction using an RGB camera on maize and peanut plantation", E3S Web of Conferences, pp. 1-6, 2023. https://doi.org/10.1051/e3sconf/202346701031
- [39] F. J. Diaz, A. Ahmad, L. Parra, S. Sendra and J. Lloret, "Low-Cost Optical Sensors for Soil Composition Monitoring", *Sensors*, vol. 24, no. 4, pp. 1-20, 2024. https://doi.org/10.3390/s24041140